Revisiting Blob Theory for DNA Diffusivity in Slitlike Confinement

Liang Dai,[1] Douglas R. Tree,[2] Johan R. C. van der Maarel,[1,3] Kevin D. Dorfman,[2] and Patrick S. Doyle[1,4,*]

[1]BioSystems and Micromechanics IRG, Singapore-MIT Alliance for Research and Technology Centre, Singapore 117543, Singapore
[2]Department of Chemical Engineering and Materials Science, University of Minnesota, Minneapolis, Minnesota 55455, USA
[3]Department of Physics, National University of Singapore, Singapore 117551, Singapore
[4]Department of Chemical Engineering, Massachusetts Institute of Technology (MIT), Cambridge, Massachusetts 02139, USA
(Received 14 December 2012; published 19 April 2013)

Blob theory has been widely applied to describe polymer conformations and dynamics in nanoconfinement. In slit confinement, blob theory predicts a scaling exponent of 2/3 for polymer diffusivity as a function of slit height, yet a large body of experimental studies using DNA produce a scaling exponent significantly less than 2/3. In this work, we develop a theory that predicts that this discrepancy occurs because the segment correlation function for a semiflexible chain such as DNA does not follow the Flory exponent for length scales smaller than the persistence length. We show that these short length scale effects contribute significantly to the scaling for the DNA diffusivity, but do not appreciably affect the scalings for static properties. Our theory is fully supported by Monte Carlo simulations, quantitative agreement with DNA experiments, and the results reconcile this outstanding problem for confined polymers.

DOI: 10.1103/PhysRevLett.110.168105 PACS numbers: 87.15.ak, 87.14.gk, 87.15.hg

The conformation and dynamics of single DNA molecules in confinement have been extensively studied, facilitated by nanofabrication techniques capable of manufacturing devices with well-defined canonical geometries and direct visualization of single DNA via fluorescence microscopy. Practically, the understanding of DNA physics in confinement is vital for the development of nanodevices for genome analysis [1–4]. Moreover, simulations and experiments of DNA in confinement have been used to critically examine classic and long-existing theories in polymer physics.

Proposed by de Gennes [5], blob theory has been applied to predict the static and dynamic scaling behavior of single polymers when varying the confining dimension, e.g., the nanochannel diameter [6,7] or the nanoslit height [8–11]. In slitlike confinement (two parallel plates), blob theory predicts a scaling of DNA extension with respect to the slit height of $R_{\parallel} \sim H^{1/4}$, which agrees with experiments [9,10] and simulations [11]. Despite the success of blob theory in predicting scalings for static properties, significant discrepancies exist between blob theory and the results of experiments and simulations for dynamic scalings: blob theory yields a scaling for diffusivity versus slit height of $D \sim H^{2/3}$, which is substantially larger than the scaling exponent seen in experiments [8,10,12–14] and simulations [15].

In this work, we reconcile the predictions of blob theory and experimental data by developing a modified theory that approximately accounts for the pair correlation of DNA segments at length scales smaller than the persistence length. While pair correlations below the persistence length have little effect on static scalings, they dramatically affect the diffusivity. By accounting for the difference between the DNA pair correlations below the persistence length, we obtain the excellent agreement between theory and experiment seen in Fig. 1.

Let us first recall the classic blob theory arguments for the scaling of DNA diffusivity in slits for the de Gennes regime ($L_p \ll H \ll R_{g,\mathrm{bulk}}$, with persistence length L_p and DNA bulk radius of gyration $R_{g,\mathrm{bulk}}$). Within the slit, DNA is represented by a series of self-avoiding blobs, each with diameter equal to the height H. Using Flory scaling [16], the contour length within a blob is

$$L_{\mathrm{blob}} \sim H^{5/3} L_p^{-1/3} w^{-1/3}, \tag{1}$$

where w is the effective chain width. Here, we use a simple Flory exponent of 3/5. (The precise value [17] is 0.5877 ± 0.0006.) The number of blobs is $N_{\mathrm{blob}} = L/L_{\mathrm{blob}}$, where L

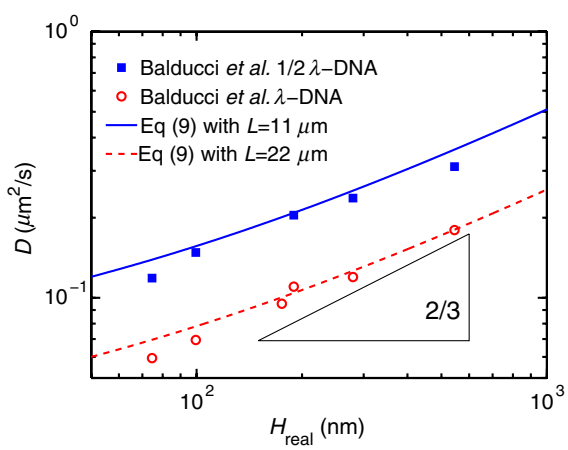

FIG. 1 (color online). Diffusivity as a function of slit height. The symbols are from previous experiments [8] for both λ-DNA and 1/2 λ-DNA. The two lines are calculated from Eq. (9) using the prefactor $c_2 = 1.68$. The triangle indicates the de Gennes scaling of 2/3.

is the contour length. In the Zimm model [18], the polymer in each blob is hydrodynamically coupled to its entrained solvent, resulting in a drag force on each blob proportional to H. The resulting scaling of diffusivity is $D \sim 1/(N_{\rm blob}H) \sim H^{2/3}L_p^{-1/3}w^{-1/3}L^{-1}$.

To understand why the classic blob theory does not capture experimental data, we need to consider a more detailed approach which accounts for correlations at the persistence length scale. The DNA diffusivity in slits is determined by hydrodynamic interaction between DNA segments. Here, hydrodynamic interaction refers to the force exerted on a particle due to the flow induced by the movement of another particle. The diffusivity in slits is approximated [19] as

$$D = \frac{k_B T}{L}\int_0^{H/2} h(r)\Omega(r)dr, \tag{2}$$

where $k_B T$ is the thermal energy, $\Omega(r) = 1/(6\pi r\eta)$ is the angle-preaveraged Oseen tensor in free solution, η is the viscosity of the solvent, and $h(r) \equiv 4\pi r^2 L_p g(r)$ is a dimensionless form of the pair correlation function $g(r)$. Based on Eq. (1), the dimensionless pair correlation used in the classic blob theory is

$$h(r) = c_1 r^{2/3}L_p^{-1/3}w^{-1/3}, \tag{3}$$

where c_1 is a prefactor. After substituting this expression into Eq. (2), the resulting diffusivity is

$$D_1 = c_2 H^{2/3}L_p^{-1/3}w^{-1/3}D_0, \tag{4}$$

where

$$D_0 = k_B T/(6\pi\eta L) \tag{5}$$

is the Rouse diffusivity and c_2 is a prefactor that corrects for the approximation of a free-solution Oseen tensor in Eq. (2). Note that applying the precise Flory exponent of 0.5877 yields the scaling $D_1 \sim H^{0.7015}$.

As expected, this calculation reproduces the result cited by many authors [8,10,12]. However, it fails to explain the experimental data because the Flory pair correlation function is used throughout the entire domain in the integral of Eq. (2). DNA behaves like a stiff rod below the persistence length, so we propose modifying the pair correlation with the approximate form:

$$h(r) = \begin{cases} 2 & r < L_p/2 \\ c_1 r^{2/3}L_p^{-1/3}w^{-1/3} & r \geq L_p/2. \end{cases} \tag{6}$$

This modified pair correlation function minimally affects the static properties of DNA in slits, such as the scaling of DNA extension. Using blob theory and Eq. (1), the in-plane DNA extension is determined as $R_{||} \approx HN_{\rm blob}^{3/4} = H(L/L_{\rm blob})^{3/4} \sim H^{-1/4}$. If the modified $h(r)$ is considered, the calculation of $L_{\rm blob}$ is broken up into two integrals:

$$L_{\rm blob} = \int_0^{L_p/2} h(r)dr + \int_{L_p/2}^{H/2} h(r)dr. \tag{7}$$

Substituting Eq. (6), the above equation becomes

$$L_{\rm blob} = \begin{cases} H & H < L_p \\ c_1\frac{3}{5}\left[\left(\frac{H}{2}\right)^{5/3} - \left(\frac{L_p}{2}\right)^{5/3}\right](L_p w)^{-1/3} + L_p & H \geq L_p. \end{cases} \tag{8}$$

For the de Gennes regime, where H is always at least a few times L_p, this modification usually causes only a few percent change in $L_{\rm blob}$. As a result, the scaling exponent of $R_{||}$ versus H will be very close to the value $1/4$ predicted by classic blob theory [10,11].

To confirm this conjecture, we used Monte Carlo simulations for DNA in slits [11]. In the simulation, DNA is modeled as a chain of N_b beads connected by $(N_b - 1)$ inextensible bonds of length l_B, corresponding to a contour length $L = (N_b - 1)l_B$. Three types of interactions are considered: hard-core repulsions between DNA beads, hard-core repulsions between DNA beads and slit walls, and bending energies between adjacent bonds. The hard-core diameter of the bead w is set to equal the bond length l_B. The bending rigidity is set to reproduce the persistence length L_p of 50 nm. The chain width is 5 nm and the contour length is 8 μm ($N_b = 1601$ beads). The simulation starts from a random conformation. In each Monte Carlo cycle, we perform either one crankshaft move or one reptation move (randomly picking the type of move). Each chain is allowed to equilibrate for 10^8 steps. After equilibration, we perform more than 10^9 steps, recording one configuration every 10^6 steps for data analysis.

We used the simulation data to estimate the contour length $L_{\rm blob}$ inside a spherical blob whose diameter equals the slit height. Note that the slit heights H in all figures are always the effective slit height, i.e., the real slit height $H_{\rm real}$ minus the chain width w, because this effective slit height is consistent with the slit height used in theoretical predictions. Recall that $L_{\rm blob}$ corresponds to the integral of $h(r)$. For each bead in a given DNA configuration, we counted how many beads are located within the distance of $H/2$. Then, we multiply this number with the bond length to obtain $L_{\rm blob}$. Figure 2 shows $L_{\rm blob}$ as a function of slit height. The simulation results with $L_p = 50$ nm are compared to Eq. (8) using a fit value of $c_1 = 2.8$. We note that although a simple piecewise function is used in Eq. (8), good agreement is obtained all through the Odijk and de Gennes regimes. There are minor discrepancies when $H \approx L_p$, where DNA behaves as neither a stiff rod nor a long chain. The modification of $h(r)$ leads to only a few percent change of $L_{\rm blob}$ when $H > 2L_p = 100$ nm. As a result, considering the subpersistence behavior of $h(r)$ has a negligible effect on $L_{\rm blob}$ as well as the scaling of DNA extension when slit height is a few times the persistence

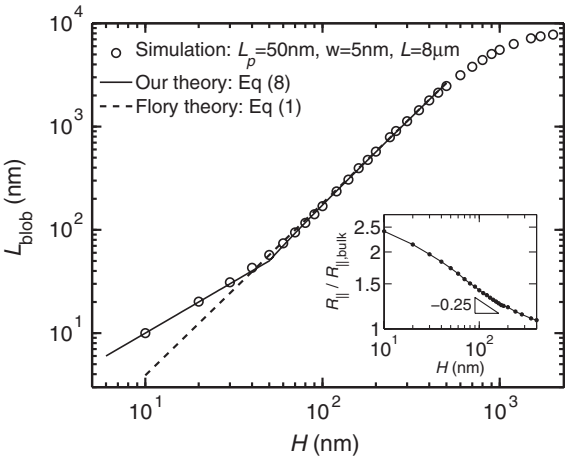

FIG. 2. The contour length inside a blob as a function of slit height. The solid line is calculated from Eq. (8) using $L_p = 50$ nm, $w = 5$ nm, and a fit value $c_1 = 2.8$. The dashed line is the result from classic blob theory, Eq. (1). The statistical errors are less than the symbol sizes. The inset plot shows the normalized in-plane radius of gyration as a function of slit height in simulations. The triangle indicates the de Gennes scaling of -0.25.

length. Indeed, the best power-law fit to the in-plane extension in the de Gennes regime [11] yields an exponent of -0.249 ± 0.010, as shown in the inset of Fig. 2 (also see Supplemental Material [20]). This exponent is very close to $-1/4$ predicted by the classic blob theory.

While the modified pair correlation function in Eq. (6) has minimal impact on the scaling for the size of the confined chain, it has a much stronger impact on the diffusivity because $\Omega(r) \sim r^{-1}$ in Eq. (2), which dramatically enhances the importance of the short-scale property of $h(r)$. Substituting Eq. (6) into Eq. (2), the diffusivity becomes

$$D = D_1 + D_2 - D_3, \tag{9}$$

where

$$D_2 \approx 2\ln(L_p/a)D_0, \tag{10}$$

$$D_3 = c_2(L_p/w)^{1/3}D_0. \tag{11}$$

The terms D_2 and $(D_1 - D_3)$ correspond to the integral over the intervals $[0, L_p/2]$ and $[L_p/2, H/2]$ in Eq. (2), respectively. In Eq. (10), a is the hydrodynamic radius of the chain. In computing D_2, we regularized the integral to remove the singularity (see Supplemental Material [20]). Equation (10) approximately corresponds to the diffusivity of a randomly oriented rod with the length L_p and the radius a [21–23]. Owing to the sharp crossover between forms of $h(r)$ in Eq. (6), it would be inappropriate to regard c_2 as a universal prefactor. Rather, we would expect that c_2 will have a slight dependence on the ratio L_p/w that arises from the details of the crossover from rodlike correlations to real chain correlations over the length scale of the slit.

Our results so far already start to explain the deviation between experiments and classic blob theory. Equation (9) differs from Eq. (4) by two additional terms, D_2 and $-D_3$. Note that $(D_2 - D_3)$ is positive and independent of H; i.e., the scaling exponent is zero. The mixture of two scaling exponents, $D_1 \sim H^{2/3}$ and $(D_2 - D_3) \sim H^0$, results in an apparent exponent less than $2/3$. This finding qualitatively agrees with experimental results [8,10,12–14].

To obtain the quantitative results seen in Fig. 1, we need to provide values for the hydrodynamic radius a appearing in Eq. (10) and the prefactor c_2 appearing in Eqs. (4) and (11). We first set $a = 1.25$ nm, which was determined from sedimentation data by Yamakawa and Fujii [22]. To obtain c_2, we fit the prediction of our theory to the diffusion coefficient obtained from Monte Carlo sampling of

$$D_{\rm sim} = \frac{k_B T}{N_b^2}\sum_{i,j}^{N_b}\left[\frac{\delta_{ij}}{6\pi\eta a_{\rm sim}}\mathbf{I} + \mathbf{\Omega}^{\rm slit}(\mathbf{r}_{ij})\right], \tag{12}$$

following the approach used in previous work [19,24]. The first term is the Stokes friction on each bead, which includes a parameter $a_{\rm sim}$. Since the simulation model is discrete, the hydrodynamic radius used in the simulations should differ from the one used in a continuous model (see Supplemental Material [20]). For the touching bead model we used here, the value $a_{\rm sim} = 1.38$ nm leads to simulated DNA diffusivities in free solution that match experimental data over a large range of DNA lengths [19,25]. The second term is the sum of the hydrodynamic interactions between beads in the presence of slit walls, which is calculated from the analytic solution of the Stokeslet in slits [26] (see Supplemental Material [20]).

The normalized (dimensionless) diffusivities calculated from simulations are shown in Fig. 3. The best power-law fit to the simulation data points in the region $2L_p < H < R_{g,\rm bulk}$ (blue filled circles) yields an apparent scaling exponent of 0.523. This exponent is close to most experiments [8,10,12], but less than the value $2/3$ predicted by classic blob theory (dashed black line). The solid (red) line is calculated from Eq. (9) using the best fit to the filled (blue) circles, giving a value of the prefactor $c_2 = 1.68$, in very good agreement with the simulations.

Our theory is only valid for the de Gennes regime. In thin slits with $H < L_p$, the angled averaged free-solution Oseen tensor is no longer a good approximation in Eq. (2) as hydrodynamics will become partially screened near the channel boundaries. Furthermore, in thin slits, chain segments tend to align with slit walls, and this alignment also affects hydrodynamic interactions. As H increases, Eq. (9) approaches the diffusivity scaling of classic blob theory, indicating a vanishing contribution of subpersistence length conformations to overall diffusivity for large slit heights. The simulation data for our 8 μm chain, naturally, follow neither our modified theory nor blob theory after the slit height passes 1 μm in size because the chain

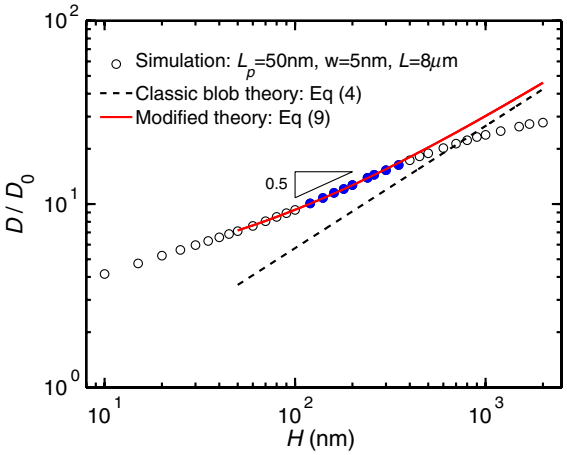

FIG. 3 (color online). Normalized DNA diffusivity as a function of slit height. The filled circles are located in $2L_p < H < R_{g,\mathrm{bulk}}$. The fit value of the prefactor c_2 in Eq. (9) is 1.68. For the parameters used in our simulations, the correlation time for the Kirkwood diffusivity is around 10^6 steps (see Supplemental Material [20]). The statistical errors are less than the symbol sizes.

diffusivity is transitioning to its bulk value. Also, note that the diffusivity is normalized with the Rouse diffusion coefficient, so the dimensionless diffusivity in an infinitely wide slit is not unity.

We are now in a position to compare our theoretical predictions with experimental results by Balducci *et al.* [8], as shown in Fig. 1. The parameters used for the theoretical predictions follow the experimental condition: $T = 22.5\,^\circ\mathrm{C}$, $\eta = 1.1$ cp, and $L = 22\ \mu$m (YOYO-labeled λ-DNA) or $L = 11\ \mu$m (YOYO-labeled 1/2 λ-DNA). Note that the DNA contour length is increased 38% by YOYO labeling at a ratio of 1 dye/4 base pairs [27–30]. We set the effective chain width to $w = 5$ nm, which is estimated by Balducci *et al.* [8]. The persistence length is set to 50 nm [27,31]. Using these parameters, Eq. (9) agrees with the experimental results in moderate confinement in Fig. 1 with no adjustment of the the prefactor $c_2 = 1.68$, which was obtained from the independent comparison to simulations.

Classic blob theory only gives the asymptotic behavior for the diffusivity scaling, as demonstrated by the dashed and solid lines in Fig. 3. We will now estimate at what slit height and contour length the scaling of diffusivity becomes sufficiently close to the de Gennes scaling of 2/3. We define the apparent scaling exponent as the slope of the D-H curve in the log-log plot. The relative deviation of the slope from the de Gennes scaling $\epsilon \equiv (2/3 - \mathrm{slope})/(2/3)$ can be determined from Eq. (9). For a given value of ϵ, the corresponding slit height is the solution of $D_1 = (1 - \epsilon)D$ for H. Picking a 5% error, $\epsilon = 0.05$, yields $H = 4.3\ \mu$m. Using Eq. (8), the value of L_{blob} is approximately 100 μm. If we assume that the application of blob theory requires at least five blobs, then the minimum contour length of DNA is about 500 μm ($\sim$1100 kbp) to observe an exponent close to the de Gennes scaling for diffusivity. This value is 1 order of magnitude greater than the contour length of DNA used in previous experiments [8,10,12–14]. As a result, interpretation of DNA dynamics in microfluidic and nanofluidic devices nearly always requires modification of classic blob theory.

In addition to resolving the long-standing mystery regarding observed scalings of DNA diffusivity in confinement, this work deepens our fundamental understanding of statics and dynamics of confined semiflexible chains. The scaling behaviors in confinement have been traditionally interpreted using the de Gennes blob theory. It is very intriguing that this classic theory works well for statics (thermodynamics) but not for dynamics (hydrodynamics). Our analysis gives a straightforward explanation related to a correction to the pair correlation at short length scales. Dynamics are sensitive to short length scale chain statistics due to the 1/(distance) scaling of the hydrodynamic interaction tensor which weights the interactions. However, statics lack this nonlinear weighting and hence are more forgiving to slight modifications of short length scale pair correlations. Looking forward, we expect that similar arguments may be applied to resolve the difference in diffusivity scaling exponents between blob theory ($\nu = 2/3$) and simulation [19,24,32] ($\nu < 2/3$) in square-channel ("tubes") confinement. Furthermore, other dynamical properties, e.g., the relaxation time, are also expected to deviate from the classic blob theory.

In conclusion, we find that the classic blob theory should be modified to include the short-scale pair correlation when applied to the dynamics of semiflexible polymers in confinement. Via modification of the subpersistence pair correlation, we have reconciled DNA experiments and simulation results with blob theory of polymers in slitlike confinement. This modification is necessary to interpret confined semiflexible polymer dynamics.

This research was supported by the National Research Foundation Singapore through the Singapore MIT Alliance for Research and Technology's research programme in BioSystems and Micromechanics, the National Science Foundation (CBET-0852235), and National Institutes of Health (R01-HG005216).

*pdoyle@mit.edu

[1] J. O. Tegenfeldt *et al.*, Proc. Natl. Acad. Sci. U.S.A. **101**, 10 979 (2004).
[2] D. Stein, F. H. J. van der Heyden, W. J. A. Koopmans, and C. Dekker, Proc. Natl. Acad. Sci. U.S.A. **103**, 15 853 (2006).
[3] K. Jo, D. M. Dhingra, T. Odijk, J. J. de Pablo, M. D. Graham, R. Runnheim, D. Forrest, and D. C. Schwartz, Proc. Natl. Acad. Sci. U.S.A. **104**, 2673 (2007).
[4] W. Reisner, N. B. Larsen, H. Flyvbjerg, J. O. Tegenfeldt, and A. Kristensen, Proc. Natl. Acad. Sci. U.S.A. **106**, 79 (2009).

[5] P.-G. de Gennes, *Scaling Concepts in Polymer Physics* (Cornell University, Ithaca, 1979).
[6] W. Reisner, K. Morton, R. Riehn, Y. Wang, Z. Yu, M. Rosen, J. Sturm, S. Chou, E. Frey, and R. Austin, Phys. Rev. Lett. **94**, 196101 (2005).
[7] Y. Wang, D. R. Tree, and K. D. Dorfman, Macromolecules **44**, 6594 (2011).
[8] A. Balducci, P. Mao, J. Han, and P. S. Doyle, Macromolecules **39**, 6273 (2006).
[9] D. J. Bonthuis, C. Meyer, D. Stein, and C. Dekker, Phys. Rev. Lett. **101**, 108303 (2008).
[10] J. Tang, S. L. Levy, D. W. Trahan, J. J. Jones, H. G. Craighead, and P. S. Doyle, Macromolecules **43**, 7368 (2010).
[11] L. Dai, J. J. Jones, J. R. C. van der Maarel, and P. S. Doyle, Soft Matter **8**, 2972 (2012).
[12] E. A. Strychalski, S. L. Levy, and H. G. Craighead, Macromolecules **41**, 7716 (2008).
[13] H. Uemura, M. Ichikawa, and Y. Kimura, Phys. Rev. E **81**, 051801 (2010).
[14] P.-K. Lin, J.-F. Chang, C.-H. Wei, P. H. Tsao, W. S. Fann, and Y.-L. Chen, Phys. Rev. E **84**, 031917 (2011).
[15] Y.-L. Chen, M. D. Graham, J. J. de Pablo, G. C. Randall, M. Gupta, and P. S. Doyle, Phys. Rev. E **70**, 060901 (2004).
[16] P. J. Flory, J. Chem. Phys. **10**, 51 (1942).
[17] B. Li, N. Madras, and A. J. Sokal, J. Stat. Phys. **80**, 661 (1995).
[18] B. H. Zimm, J. Chem. Phys. **24**, 269 (1956).
[19] D. R. Tree, Y. Wang, and K. D. Dorfman, Phys. Rev. Lett. **108**, 228105 (2012).
[20] See Supplemental Material at http://link.aps.org/supplemental/10.1103/PhysRevLett.110.168105 for effect of slit walls on hydrodynamic interaction; DNA diffusivity contributed by short-scale hydrodynamic interaction; effect of chain discretization on the calculation of diffusivity; scaling of DNA extension in slits; and correlation of the diffusivity in Monte Carlo simulation.
[21] G. K. Batchelor, J. Fluid Mech. **44**, 419 (2006).
[22] H. Yamakawa and M. Fujii, Macromolecules **6**, 407 (1973).
[23] D. F. Katz, J. R. Blake, and S. L. Paveri-Fontana, J. Fluid Mech. **72**, 529 (2006).
[24] R. M. Jendrejack, D. C. Schwartz, M. D. Graham, and J. J. de Pablo, J. Chem. Phys. **119**, 1165 (2003).
[25] R. M. Robertson, S. Laib, and D. E. Smith, Proc. Natl. Acad. Sci. U.S.A. **103**, 7310 (2006); D. E. Smith, T. T. Perkins, and S. Chu, Macromolecules **29**, 1372 (1996); S. S. Sorlie and R. Pecora, Macromolecules **23**, 487 (1990).
[26] N. Liron and S. Mochon, J. Eng. Math. **10**, 287 (1976).
[27] K. Güther, M. Mertig, and R. Seidel, Nucleic Acids Res. **38**, 6526 (2010).
[28] O. B. Bakajin, T. A. J. Duke, C. F. Chou, S. S. Chan, R. H. Austin, and E. C. Cox, Phys. Rev. Lett. **80**, 2737 (1998).
[29] B. Ladoux and P. S. Doyle, Europhys. Lett. **52**, 511 (2000).
[30] K. D. Dorfman, S. B. King, D. W. Olson, J. D. P. Thomas, and D. R. Tree, Chem. Rev., doi: 10.1021/cr3002142 (2012).
[31] C. U. Murade, V. Subramaniam, C. Otto, and M. L. Bennink, Nucleic Acids Res. **38**, 3423 (2010).
[32] J. L. Harden and M. Doi, J. Phys. Chem. **96**, 4046 (1992).

Supplemental material to:
Revisiting blob theory for DNA diffusivity in slitlike confinement

Liang Dai[1], Douglas R. Tree[2], Johan R. C. van der Maarel[1,3], Kevin D. Dorfman[2], and Patrick S. Doyle[1,4*]

[1]*BioSystems and Micromechanics IRG, Singapore-MIT Alliance for Research and Technology Centre, Singapore 117543,*

[2]*Department of Chemical Engineering and Materials Science, University of Minnesota, Minneapolis, MN 55455,*

[3]*Department of Physics, National University of Singapore, Singapore 117551*

[4]*Department of Chemical Engineering, Massachusetts Institute of Technology (MIT), Cambridge, MA 02139*

*pdoyle@mit.edu

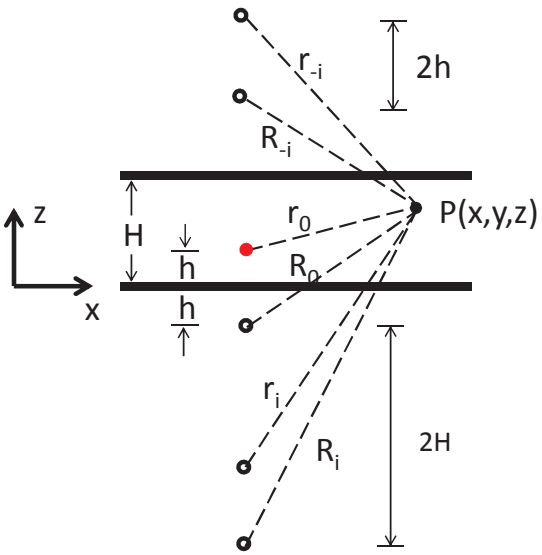

FIG. S1. (Color online) A schematic for the analytic solution of Stokeslet in a slit (side view). Reproduced from [1]. The two thick lines represent the two slit walls. A point unit force is applied at the position of red dot. We solve the velocity at the point of **P**(x, y, z). The open circles are the images of red dot.

I. THE EFFECT OF SLIT WALLS ON HYDRODYNAMIC INTERACTION

This section is to describe the method of calculating the hydrodynamic interaction $\mathbf{\Omega}^{\text{slit}}(\mathbf{r_i}, \mathbf{r_j})$ in Eq. (12). The physical meaning of $\mathbf{\Omega}^{\text{slit}}(\mathbf{r_i}, \mathbf{r_j})$ is the velocity at the point $\mathbf{r_j}$ induced by a unit point force at the point $\mathbf{r_i}$ in a slit. We use U_j^k to represent the (k,j) component of $\mathbf{\Omega}^{\text{slit}}(\mathbf{r_i}, \mathbf{r_j})$, which corresponds to the velocity in j-direction induced by a unit point force in k-direction in slit. We calculate U_j^k using the analytic solution of the Stokes flow for a stokeslet between two parallel flat plates [1]. Figure S1 shows the schematic for the analytic solution. The analytic solution is obtained by image technique and considering the no-slip condition on the two plates. The red dot is the position of the applied force, and the open circles are the images of the red dot assuming the two slit walls are two mirrors. We calculate the velocity at the point of $\mathbf{P}(x, y, z)$. The value of U_j^k depends on the slit height H, the height h of the point $\mathbf{r_i}$, and the relative position of two points $\mathbf{r} = \mathbf{r_j} - \mathbf{r_i}$. So we write U_j^k as $U_j^k(H, h, x, y, z)$. The expression of U_j^k is shown by the below equations. We only show the equations when k and j correspond to $X-$ or $Y-$ direction, because $Z-$direction components of U_j^k is not relevant to the in-plane diffusivity.

$$U_j^k(H,h,x,y,z) = u_j^k + v_j^k + w_j^k, \tag{S1}$$

$$u_j^k = \frac{1}{8\pi\eta}\left(\frac{1}{r_0}\delta_{jk} - \frac{r_{0j}r_{0k}}{r_0^3}\right), \tag{S2}$$

$$v_j^k = \frac{1}{8\pi\eta}\sum_{n=-\infty,\neq 0}^{\infty}\left[\left(\frac{1}{r_0}-\frac{1}{R_0}\right)\delta_{jk} + \frac{r_{nj}r_{nk}}{r_n^3} - \frac{R_{nj}R_{nk}}{R_n^3}\right], \tag{S3}$$

$$w_j^k = -\frac{1}{4\pi\eta}\frac{\partial}{\partial r_k}\frac{r_j}{\sqrt{x^2+y^2}}\int_0^\infty \xi J_1\left(\xi\sqrt{x^2+y^2}\right)A_1(\xi)\mathrm{d}\xi, \tag{S4}$$

where

$$\mathbf{r}_n = (r_{n1}, r_{n2}, r_{n3}) = (x, y, z-h+2nH), \tag{S5}$$

$$\mathbf{R}_n = (R_{n1}, R_{n2}, R_{n3}) = (x, y, z+h+2nH), \tag{S6}$$

$$k = x, y\ ;\quad j = x, y\ ;\quad n = 0, \pm1, \pm2,\ ... \tag{S7}$$

$$A_1(\xi) = \left[\sinh^2\xi H - (\xi H)^2\right]^{-1}(T_1+T_2+T_3-T_4), \tag{S8}$$

with

$$T_1 = \xi hHz\sinh\xi(H-z)\sinh\xi(H-h), \tag{S9}$$

$$T_2 = z\left[h\sinh\xi H\cosh\xi(H-z-h) - H\sinh\xi h\cosh\xi z\right], \tag{S10}$$

$$T_3 = \xi Hz\sinh\xi H\cosh\xi(H-z)\frac{\mathrm{d}}{\mathrm{d}\xi}\frac{\sinh\xi(H-h)}{\sinh\xi H}, \tag{S11}$$

$$T_4 = H\sinh\xi z\left[\sinh\xi H\frac{\mathrm{d}}{\mathrm{d}\xi}\frac{\sinh\xi h}{\sinh\xi H} + \xi H\frac{\mathrm{d}}{\mathrm{d}\xi}\frac{\sinh\xi(H-h)}{\sinh\xi H}\right]. \tag{S12}$$

In Eq. (S1), the total velocity consists of three parts. The first part u_j^k is the stokeslet in free solution for the red dot in Fig. S1. The second part v_j^k is the Stokeslet for the open circles in Fig. S1. The sum of the first and the second parts satisfies the no-slip condition in X- and Y- directions. The third part w_j^k is included to satisfy the no-slip condition in Z-direction. In Eq. (S4), $J_1(x)$ is the Bessel function of the first kind.

Figure S2 shows the direction of flow field solved using Eq. (S1) when $h = z = H/2$. The pattern of flow field is similar for other values of h and z. The direction of flow turns back at the both sides (top and bottom) of the applied force.

When the in-plane distance is much larger than slit height, *i.e.* $\sqrt{x^2+y^2} \gg H$, the velocity can be approximated as

$$U_j^k = -\frac{3z}{2\pi\eta}\frac{h}{H}\left(1-\frac{z}{H}\right)\left(1-\frac{h}{H}\right)\frac{\partial}{\partial r_k}\left(\frac{r_j}{x^2+y^2}\right), \tag{S13}$$

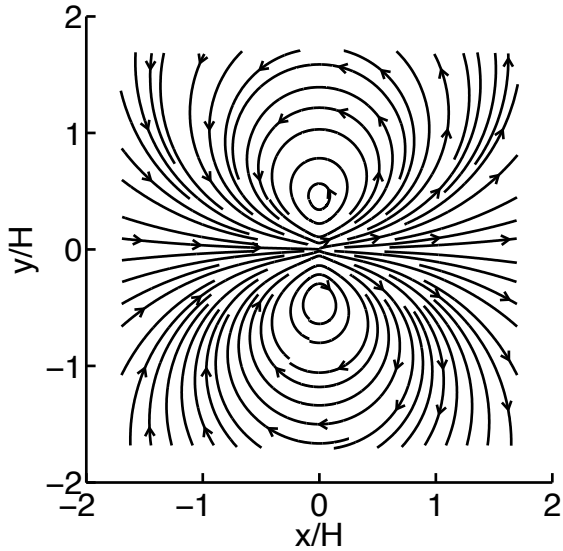

FIG. S2. The in-plane flow field induced by a point force in a slit for the parameters $h = z = H/2$.

where $\mathbf{r} = (x, y, z)$. This far field approximation has been used in our calculation of diffusivity when $\sqrt{x^2 + y^2} > 10H$.

II. DNA DIFFUSIVITY CONTRIBUTED BY SHORT-SCALE HYDRODYNAMIC INTERACTION

As shown by Eq. (6), we modify the pair correlation function on the sub-persistence length scale. Substituting $h(r) = 2$ and $\Omega(r) = 1/(6\pi\eta r)$ into Eq. (2) will produce a singularity. It is because the chain thickness is ignored in $\Omega(r) = 1/(6\pi\eta r)$. The thickness is crucial for the integral near $r = 0$ in Eq. (2). Following the previous study of slender body theory [2], we modify $\Omega(r)$ to be $1/(6\pi\eta\sqrt{r^2 + a^2})$. Then, D_2 in Eq. (10) is calculated as

$$D_2 = 2\,\mathrm{asinh}\left[L_p/(2a)\right] D_0 \approx 2\ln(L_p/a) D_0 \tag{S14}$$

The function $\mathrm{asinh}(x)$ approaches $\ln(2x)$ very quickly. For example, $\mathrm{asinh}(x)/\ln(2x) = 1.27$, 1.04 or 1.01, when $x = 1$, 2 or 3.

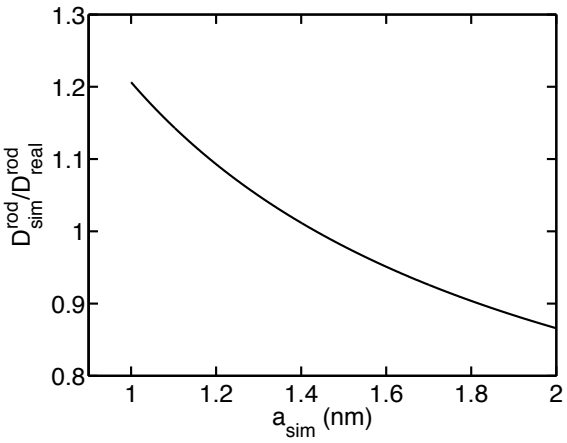

FIG. S3. The ratio of two diffusivities calculated from Eqs. (S15) and (S16) when $a = 1.25$ nm, $w = 5$ nm, $N_b = 11$ and $L = 50$ nm.

III. EFFECT OF CHAIN DISCRETIZATION ON THE CALCULATION OF DIFFUSIVITY

The simulations use a touching bead model that introduces some discretization errors. In order to match the simulations to the diffusivity of a continuous chain with hydrodynamic radius a, we need to select a somewhat larger hydrodynamic radius a_{sim} in the simulations.

For example, consider the role of discretization in a touching bead model containing one persistence length ($N_b = 11$ beads of size $w = 5$ nm) arranged on a straight line. The corresponding diffusion coefficient from the simulation is

$$D^{\text{rod}}_{\text{sim}} = \frac{k_B T}{6\pi\eta N_b w}\left[\frac{w}{a_{\text{sim}}} + \frac{1}{N_b}\sum_{i,j=1,i\neq j}^{N_b}\frac{1}{|i-j|}\right]. \tag{S15}$$

On the other hand, the diffusion coefficient for a continuous rod is derived as

$$\begin{aligned} D^{\text{rod}}_{\text{real}} =& \frac{k_B T}{6\pi\eta L^2}\int_0^L dx_1 \int_0^L dx_2 \frac{1}{\sqrt{(x_1-x_2)^2+a^2}} \\ =& \frac{k_B T}{6\pi\eta L}\left[2\,\text{asinh}\left(\frac{L}{a}\right) - 2\left(\sqrt{1+\left(\frac{a}{L}\right)^2} - \frac{a}{L}\right)\right], \end{aligned} \tag{S16}$$

following the approach by Yamakawa and Fujii [3]. In this example problem, we would want to pick a_{sim} such that the diffusion predicted by the discrete model in Eq. (S15) agrees with the continuous result in Eq. (S16). As we see in Fig. S3, these models agree with $a_{\text{sim}} = 1.434$ nm.

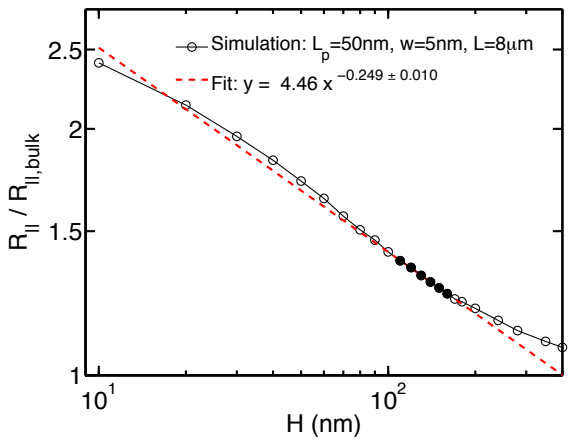

FIG. S4. (Color online) The normalized in-plane radius of gyration as a function of slit height. The filled circles are located in $2L_p < H < R_{g,bulk}/2$ according to the previous study [5]. The dashed line is the best power law fit to filled circles. The parameters in simulations are $L_p = 50$ nm, $L = 8$ μm and $w = 5$ nm.

Our simulations do not correspond to the rod-like toy model, but rather use real wormlike chains with excluded volume interactions. For the simulations, we use the value $a_{\rm sim} = 1.38$ nm, which was determined by Tree *et al.* [4] to match the DNA diffusivities in free solution produced by this simulation model to experimental data over a range of DNA lengths.

IV. SCALING OF DNA EXTENSION IN SLITS

Figure S4 shows the normalized in-plane radius of gyration as a function of slit height. According to the previous study [5], we fit the data points in $2L_p < H < R_{g,bulk}/2$. The best power law fit yields an exponent of 0.249, which is very close to $-1/4$ predicted by the classic blob theory.

V. CORRELATION OF THE DIFFUSIVITY IN MONTE CARLO SIMULATION

For every DNA configuration during simulations, we calculate the diffusivity using Eq. (12) in the main article. The diffusivity loses correlation after a certain simulation steps. We calculate the self-correlation of diffusivity as a function of simulation steps, as shown in Fig. S5. The correlation times are around 10^6 steps. Our simulation is about 10^3 times of

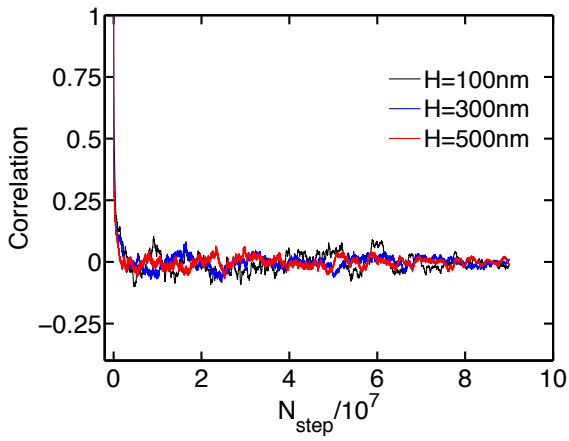

FIG. S5. (Color online) Self-correlation of diffusivity as a function of simulation steps. The parameters in simulations are $L_p = 50$ nm, $L = 8$ μm and $w = 5$ nm.

the correlation time, and the statistical errors are less than the symbols in all figures.

---

[1] N. Liron and S. Mochon, *J. Engineering Math.* **10**, 287 (1976).

[2] G.K. Batchelor, *J. Fluid Mech.* **44**, 419 (1970).

[3] H. Yamakawa and M. Fujii, *Macromolecules* **6**, 407 (1973).

[4] D. R. Tree, Y. Wang, and K. D. Dorfman, *Phys. Rev. Lett.* **108**, 228105 (2012).

[5] L. Dai, J. J. Jones, J. R. C. van der Maarel, and P. S. Doyle, *Soft Matter* **8**, 2972 (2012).